

**Edge-Plasma Heating
via Parasitic-Torsional-Mode Excitation
by Faraday-Shielded Ion-Bernstein-Wave Antennas**

Garching bei München, Federal Republic of Germany

Satish Puri

IPP 4/239

November 1989



MAX-PLANCK-INSTITUT FÜR PLASMAPHYSIK

8046 GARCHING BEI MÜNCHEN

MAX-PLANCK-INSTITUT FÜR PLASMAPHYSIK
GARCHING BEI MÜNCHEN

Edge-Plasma Heating
via Parasitic-Torsional-Mode Excitation
by Faraday-Shielded Ion-Bernstein-Wave Antennas

Satish Puri

IPP 4/239

November 1989

Die nachstehende Arbeit wurde im Rahmen des Vertrages zwischen dem Max-Planck-Institut für Plasmaphysik und der Europäischen Atomgemeinschaft über die Zusammenarbeit auf dem Gebiete der Plasmaphysik durchgeführt.

EDGE-PLASMA HEATING
VIA PARASITIC-TORSIONAL-MODE EXCITATION
BY FARADAY-SHIELDED ION-BERNSTEIN-WAVE ANTENNAS

Satish Puri

Max-Planck Institut für Plasmaphysik, EURATOM Association,
Garching bei München, Federal Republic of Germany

ABSTRACT

Presence of large- k_z spectral component in Faraday-shielded Ion-Bernstein-Wave (IBW) antennas couples a significant amount of power to the finite-temperature parasitic torsional mode. The wave transfers its energy to the plasma electrons via Landau damping. This mechanism may play a vital part in the observed background loading in IBW heating experiments. The conditions for the parasitic mode excitation are examined and the antenna loading for some idealized cases is computed. Methods for minimizing parasitic excitation are discussed.

PACS numbers: 52.50.Gj; 52.40.Db

Plasma heating using ion-Bernstein waves (IBW) has been proposed as an alternative to the fast-wave heating in the ion-cyclotron frequency regime.¹ Among the advantages is direct single pass ion heating. Possible disadvantages include coupling to impurity cyclotron harmonics near the plasma edge.¹ The recent IBW heating experiments in D3D exhibit additional anomalous background loading apparently unconnected with the excitation of the IBW itself.² A characteristic feature is the independence of the observed loading on the antenna voltage, indicative of the existence of a hitherto unsuspected linear process. Similar, though less pronounced, parasitic loading occurs in the JIPPT³, PLT⁴, and ALCATOR⁵ IBW heating experiments.

In this paper I suggest *finite-electron-temperature parasitic torsional mode* (PTM) associated with the large- k_z spectral component of a Faraday-shielded antenna as a possible mechanism for the anomalous loading. The approximate torsional wave differential equation may be expressed in the form

$$\mathcal{E}_z'' + \left[-\frac{\epsilon_z}{\epsilon_x} k_z^2 + \frac{1}{4} \left(\frac{\epsilon_x'}{\epsilon_x} \right)^2 \right] \mathcal{E}_z = \mathcal{E}_z'' + k_x^2 \mathcal{E}_z = 0, \quad (1)$$

where $\mathcal{E}_z(k_z) = \epsilon_x^{-1/2} E_z(k_z)$,

$$\epsilon_x \approx 1 + \frac{\omega_{pe}^2}{\omega_{ce}^2} - \frac{\omega_{pi}^2}{\omega^2 - \omega_{ci}^2}, \quad (2)$$

$$\epsilon_z \approx 1 - \frac{\omega_{pi}^2}{\omega^2} + 2 \frac{\omega_{pe}^2}{k_z^2 v_e^2} \left[1 + i\pi^{1/2} \zeta_e \exp(-\zeta_e^2) \right], \quad (3)$$

$\zeta = \omega/k_z v$, v is the particle thermal speed. It is assumed that $\zeta_e \ll 1$ and $\zeta_i \gg 1$. For a density gradient length l_g

$$k_x^2 = -\frac{\epsilon_z}{\epsilon_x} k_z^2 + \frac{1}{4l_g^2}. \quad (4)$$

Since $\Re[\epsilon_z] > 0$ for $\zeta_e < 1$, propagating or evanescent solutions to Eq.(1) exist for $\epsilon_x \leq 0$ accordingly as the plasma density $n_e \geq n_{LH}$, the lower-hybrid (LH) density. For the D3D IBW heating experiment in hydrogen at 38 MHz with $T_e = 10 \text{ eV}$, $Z_{eff} = 2$, one finds that $\Re[k_x^2] > 0$ for $n_e \gtrsim 2 \times 10^{16} \text{ m}^{-3}$ and $k_z \gtrsim 100 \text{ m}^{-1}$. Since both these conditions are readily satisfied in practice, the experimentally pertinent case corresponds

to the existence of propagating PTM excited by the IBW antennas. The coupled waves experience efficient Landau damping with the damping length

$$\lambda_{zi} = \frac{2\pi}{k_{zi}} \approx \sqrt{\frac{2}{\pi}} \left(\frac{m_e}{m_i} \right)^{1/2} \frac{\exp(\zeta_e^2)}{\zeta_e^2} \lambda_z . \quad (5)$$

The large k_z needed for the existence of the propagating PTM mode is provided by the closely spaced Faraday-shield rods in front of the IBW antenna. This effect is further accentuated by the Debye sheaths which redistribute the parallel electric field in narrow pulses bordering the Faraday-shield conductors. Fig.1 is an idealized representation of the electric field immediately in front of the Faraday shield. The antenna consists of two sections, each of length $2l$, excited in phase or in phase opposition, h is antenna height, $2s$ is the width of the Faraday-shield conductors, $2g$ is the gap between adjacent conductors, and $2d = \lambda_D = \epsilon_0 T_e / n_e e^2$ is the electron Debye length. The electric-field spectrum for the in-phase $(0,0)$ and out-of-phase $(0,\pi)$ excitation respectively, is given by

$$E_z(k_z) = \sum_n \frac{4dl\hat{E}}{\pi(s+g)} \frac{\sin[2(k_z - nk_{z0})l]}{2(k_z - nk_{z0})l} \frac{\sin(nk_{z0}d)}{nk_{z0}d} \cos[nk_{z0}(s+d)] , \quad (6a)$$

and

$$E_z(k_z) = \sum_n \frac{4dl\hat{E}}{\pi(s+g)} \frac{\sin^2[(k_z - nk_{z0})l]}{(k_z - nk_{z0})l} \frac{\sin(nk_{z0}d)}{nk_{z0}d} \cos[nk_{z0}(s+d)] , \quad (6b)$$

where $k_{z0} = \pi/(s+g)$ and \hat{E} is the electric-field pulse height.

The total power coupled into the PTM is given by

$$\mathbf{P} = h \int_{-\infty}^{\infty} E_z(z) H_y^*(z) dz = h \int_{-\infty}^{\infty} dz \int dk_z \int E_z(k_z) H_y^*(k'_z) \exp[i(k_z - k'_z)z] dk'_z . \quad (7)$$

The k_z integrations extend over the region $k_z^2 > 0$. Performing the z and k'_z integrations yields

$$\mathbf{P} \approx 4\pi h \int_{\frac{\omega}{v_e}}^{\sqrt{\frac{2m_i}{m_e}} \frac{\omega}{v_e}} E_z(k_z) H_y^*(k_z) dk_z . \quad (8)$$

Writing $\eta(k_z) = \Re[E_z(k_z)/H_y(k_z)]$, the real power flow becomes

$$P \approx 4\pi h \int_{\frac{\omega}{v_e}}^{\sqrt{\frac{2m_i}{m_e}} \frac{\omega}{v_e}} \frac{|E_z(k_z)|^2}{\eta(k_z)} dk_z . \quad (9)$$

Also Maxwell's equations together with Eq.(1) provide

$$\eta(k_z) = \Re \left[\frac{\eta_0 k_x}{\epsilon_z k_0} \right], \quad (10)$$

where η_0 is the free-space impedance. Assuming high- Q operation, the parasitic antenna loading resistance becomes

$$R_{PTM} \approx \frac{\omega^2 L^2}{V^2} P, \quad (11)$$

where $V = 8dl\hat{E}/(s + g)$ and L is the total antenna inductance.

I now proceed to estimate the power coupled by the antenna to the IBW. Since $\Lambda = (1/2)k_x^2 r_{ci}^2$ is well in excess of unity, the quasi-electrostatic dispersion relation may be approximated by $\epsilon_x \approx 0$, giving

$$\Lambda^{3/2} \approx \sqrt{\frac{2}{\pi}} \left(\frac{\omega_{pi}^2}{\omega^2 - \omega_{ci}^2} \right) \left(1 + \frac{\omega_{pe}^2}{\omega_{ce}^2} \right)^{-1}, \quad (12)$$

where it is assumed that $\Lambda \gg 1$ and only the fundamental cyclotron harmonic terms are retained in the expansion of ϵ_x . Since $\zeta_e \gg 1$, $\epsilon_z \approx -\omega_{pe}^2/\omega^2$. Using Eq.(10) one obtains $\eta(k_z)$. Finally, R_{IBW} is obtained from Eq.(11) and Eq.(9) using the integration range $0 < k_z < \omega/v_e$. Since the assumption $\Lambda \gg 1$ used in deriving Eq.(12) breaks down as the LH density is approached, the value of R_{IBW} found by this procedure is no longer accurate in the neighborhood of the LH density.

In the unlikely event that n_e at the antenna is below the LH density, the antenna launches the LH wave instead of the IBW. Subsequent to wave conversions, however, the LH wave is successively transformed into a plasma wave and an IBW. For the cold-plasma LH wave, $\epsilon_x > 0$, $\epsilon_z \approx -\omega_{pe}^2/\omega^2$, k_x^2 is given by

$$k_x^2 \approx \frac{\epsilon_z}{\epsilon_x} (\epsilon_x k_0^2 - k_z^2) + \frac{1}{4l_g^2}, \quad (13)$$

and $\eta(k_z)$ is obtained from Eq.(10). The integration range in Eq.(9) extends over $k_{acc} < k_z < \omega/v_e$, where $k_{acc} \approx k_0$ defines the accessibility condition for the LH wave. R_{LH} is then given by Eq.(11) in the usual manner. Finite density gradient l_g in Eq.(4) clamps a lower bound on k_x and hence on $\eta(k_z)$ for the low k_z values.

As already mentioned, for the low-density case ($n_e < n_{LH}$) PTM is evanescent from the antenna till the LH resonance ($\epsilon_x = 0$) with an evanescence length of $\lambda_{evan} \lesssim (\omega/\omega_{pe})\lambda_z$. The presence of the Landau damping term in ϵ_z could, in principle, cause energy absorption in the immediate vicinity of the antenna. However the extremely short evanescence length λ_{evan} (much shorter, in fact, than the damping length λ_x ; found for the high density case) precludes significant energy transfer to the plasma. The proper manner to proceed in this case would be to cast Eq.(1) in the form of a Whittaker equation⁶ near the LH singularity at $x = x_0$, giving

$$\mathcal{E}_z'' + \left[\frac{\alpha + \beta x}{x - x_0} + \frac{1}{4l_g^2} \right] \mathcal{E}_z = 0, \quad (14)$$

where a linear density profile in the scrape-off region is assumed. Matching the fields at the singularity and assuming that the wave propagates without reflection beyond the LH layer would determine $\eta(k_z)$ and hence the power coupled from the antenna to the plasma. However, I omit this exercise since the small PTM coupling is unlikely to play a significant role in the overall antenna performance and because the low-density case is of little relevance.

I now present computed values of the antenna loading R for parameters representative of D3D, with $s = g = 1 \text{ cm}$, $h = 16 \text{ cm}$, $l_g = 10 \text{ cm}$, $L = 0.2 \mu\text{H}$, and $f_{ci} = 19 \text{ MHz}$. The typical operating point (shown as a large black dot in the figures) is chosen to be $n_e = 10^{17} \text{ m}^{-3}$, $T_e = 10 \text{ eV}$, $T_i = 4 \text{ eV}$, $Z_{eff} = 2$, $f = 2f_{ci}$, and the gas used is hydrogen.

Figure 2 shows that although both PTM and IBW coupling improve with n_e , the PTM loading significantly exceeds the IBW loading even for unrealistically large T_i values. I have ignored the direct PTM coupling to ions in these computations. Coupling to ion PTM is small, in any case, because loading falls off with larger k_z needed for the ion modes. For very low n_e , LH dominates the antenna loading.

PTM coupling decreases with increasing T_e (Fig.3) because the k_z integration range in Eq.(9) shrinks. However, even at elevated temperatures, coupling to PTM overwhelms the IBW loading.

PTM loading at first increases with f (Fig.4) due to the enlarged integration range in Eq.(9) but subsequently starts decreasing as ϵ_x decreases. Also, increase in f raises the lower integration limit in Eq.(9) thereby excluding the lower- k_z values which contribute heavily to the PTM loading. This result suggests that one way to reduce PTM loading is to deliberately remove the low- k_z components associated with the Faraday-shield by decreasing the size and the spacing of the conductors. Fig.5 shows the rapid fall in the PTM loading as s and g are made smaller. For very low values of s and g , the PTM loading could be made less than the IBW loading. Fabricating antennas with such fine shield structures, however, may not be a practical proposition.

To summarize, it has been shown that the existence of a Faraday shield is unavoidably accompanied by the excitation of PTM which could seriously interfere with IBW heating. The foregoing results were obtained using the $(0,0)$ antenna configuration. About the only significant effect of the $(0,\pi)$ antenna geometry is a reduction in the LH coupling.

The existence of significant parasitic electron heating is consistent with the D3D observations and might be responsible for the density rise invariably associated with IBW heating. The increase in R with f is in agreement with the experiment. The insensitivity of R with respect to the magnetic field⁴ is also in accord with theoretical expectations. But the theory presented here does not account for the observed differences in the $(0,0)$ and $(0,\pi)$ loading in D3D. The absence of ion heating in D3D in contrast with the JIPPT³, PLT⁴, and ALCATOR⁵ results could conceivably be due to the larger Z_{eff} in D3D. Figure 6 shows the increase in PTM loading as a function of Z_{eff} . The impurities would conceal bulk-ion-heating effects by stripping the wave energy near the uncontained plasma edge.¹

One concludes that the present theory, though lacking in a complete description of the observed anomalous loading, clearly establishes PTM as a serious obstacle to IBW plasma heating. Whether the PTM loading can be significantly lowered through the use of finely spaced Faraday shields and cleaner plasmas or whether the effect of

PTM could be tolerated at higher plasma temperatures (that lead to an increase in the IBW loading and decrease in the PTM loading) are questions yet to be settled. Nor do these findings rule out successful IBW heating using waveguide coupling.¹ Even the troublesome impurity-harmonic coupling could be avoided by heating reactor-grade plasmas at ω_{cT} , the fundamental tritium cyclotron frequency.⁷

During the course of this work I was informed by Dr. S. C. Chiu that similar ideas regarding PTM excitation in IBW plasma heating experiments are being independently pursued by the General Atomic group in San Diego. I am much obliged to Dr. A. B. Murphy for helpful discussions during the course of this work.

References

1. S. Puri, *Phys. Fluids* **22**, 1716 (1979).
2. R. I. Pinsky, et al., in *AIP Conference Proceedings No.190*, 8th Topical Conference on Radio-Frequency Power in Plasmas, Irvine, CA, 1989, p.314.
3. M. Ono et al., *Phys. Rev. Letters* **54**, 2339 (1985).
4. J. R. Wilson, et al., *J. Nucl. Mat.* **145-147**, 616 (1987).
5. Y. Takase et al., *Phys. Rev. Letters* **59**, 1201 (1987).
6. K. G. Budden, in *Radio Waves in the Ionosphere*, Cambridge University Press, 1961, p. 476.
7. S. Puri in *Proc. 3rd Top. Conf. on Radio Frequency Plasma Heating, Pasadena, California, 1978*, edited by R. Gould (Caltech, Pasadena, CA, 1978).

Figure Captions

Fig.1 Idealized electric-field distribution immediately in front of the IBW antenna. Hatched regions corresponding to the Faraday-shield conductors are bordered by electric-field pulses of width $2d$ equal to the Debye length.

Fig.2 PTM, IBW and LH loading versus n_e . The IBW loading is shown as a function of T_i .

Fig.3 PTM loading versus T_e .

Fig.4 PTM loading versus f .

Fig.5 PTM loading versus (s, g) .

Fig.6 PTM loading versus Z_{eff} .

Figure Caption

Fig. 1 Idealized electric-field distribution immediately in front of the IBW antenna. Hatched regions corresponding to the Faraday-shield conductors are bordered by electric-field pulses of width $2d$ equal to the Debye length.

Fig. 2 PTM, IBW and LH loading versus α . The IBW loading is shown as a function of α .

Fig. 3 PTM loading versus T_e .

Fig. 4 PTM loading versus λ .

Fig. 5 PTM loading versus (λ, ν) .

Fig. 6 PTM loading versus β .

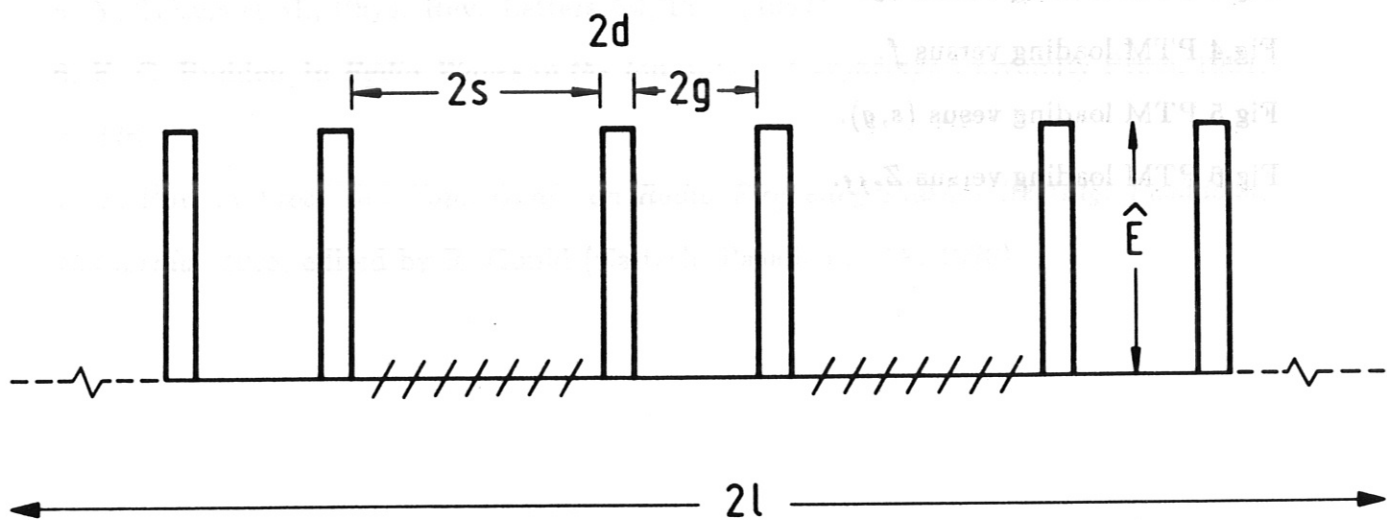


Fig.1 Idealized electric-field distribution immediately in front of the IBW antenna. Hatched regions corresponding to the Faraday-shield conductors are bordered by electric-field pulses of width $2d$ equal to the Debye length.

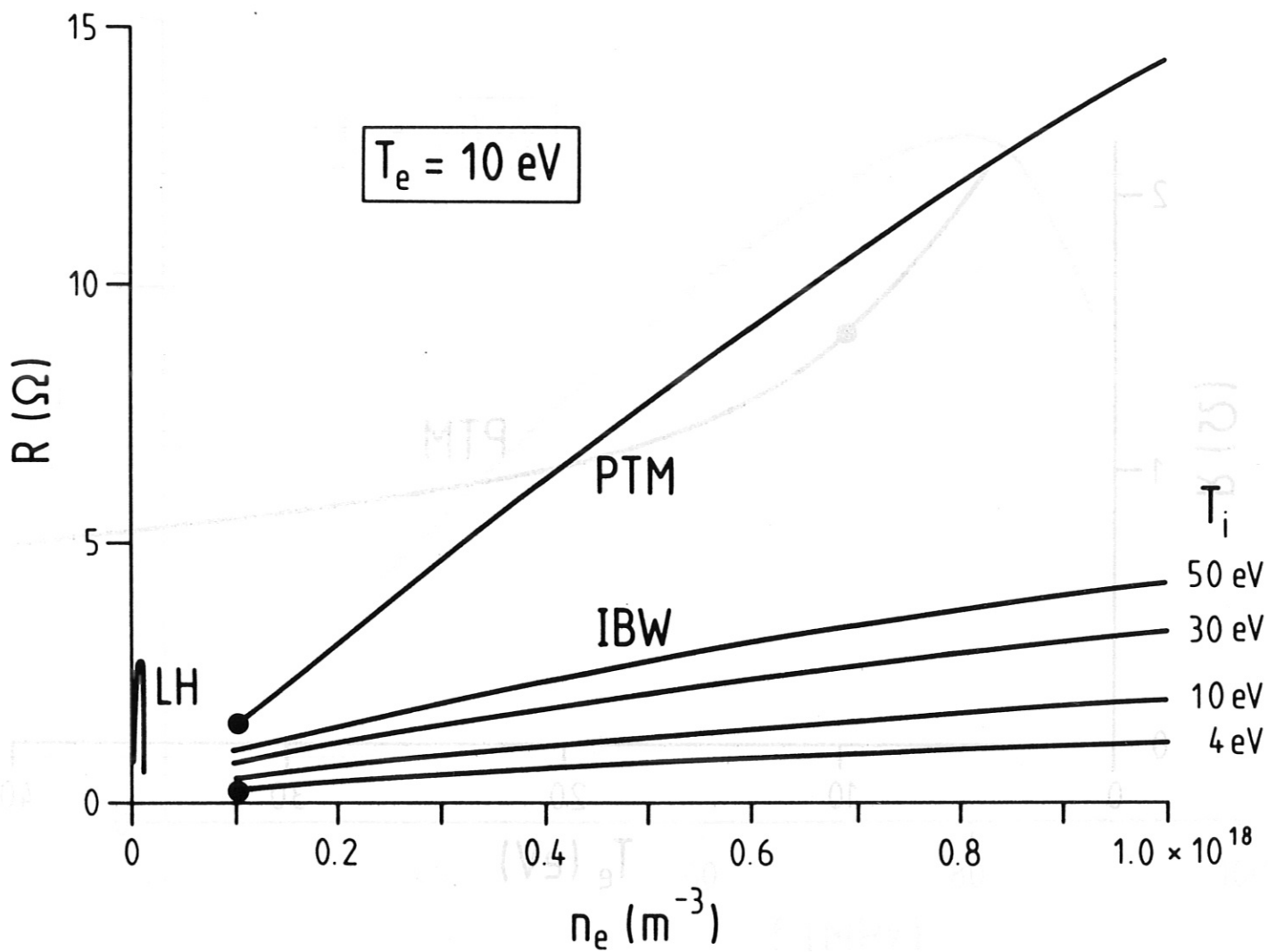


Fig.2 PTM, IBW and LH loading versus n_e . The IBW loading is shown as a function of T_i .

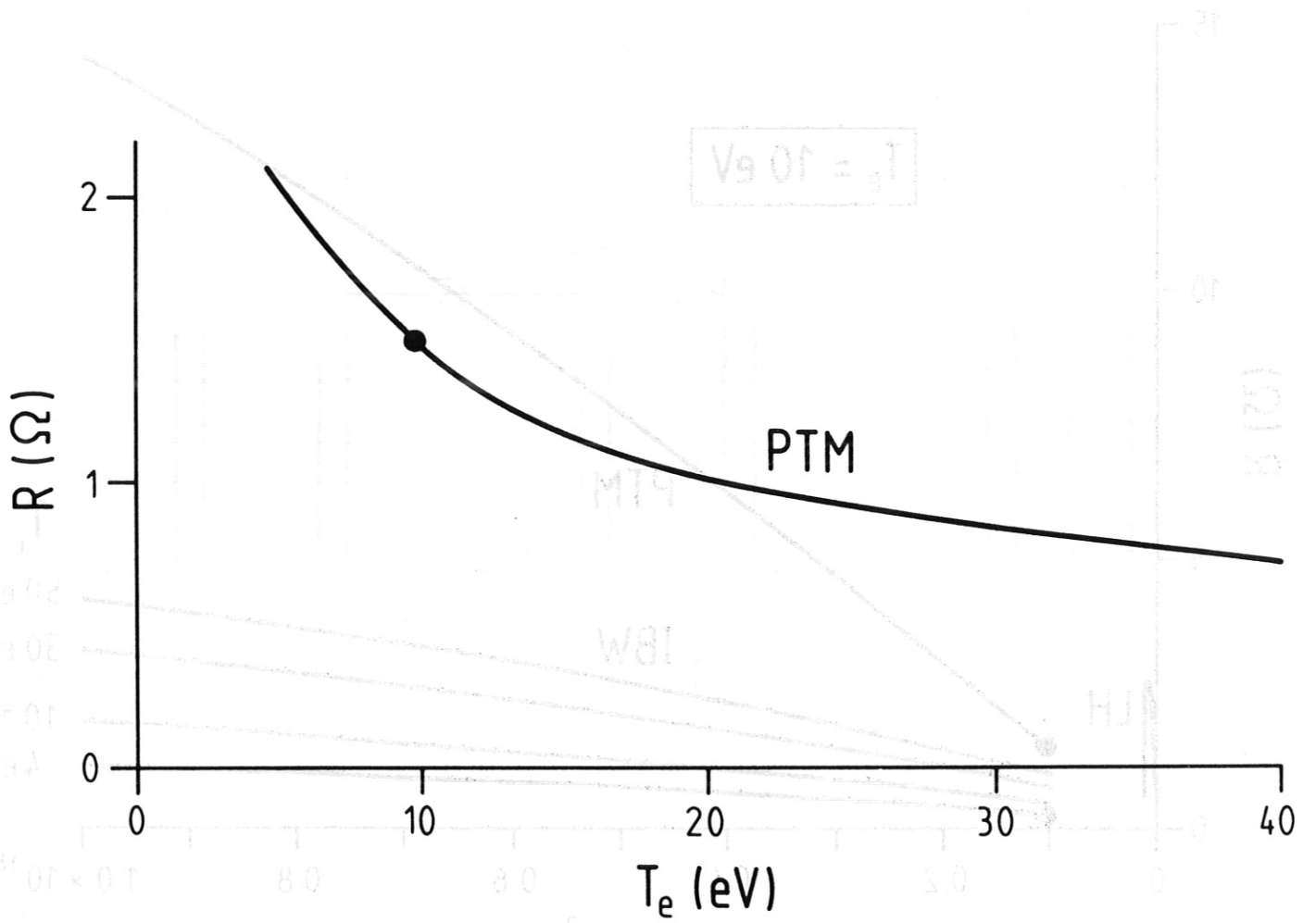


Fig.3 PTM loading versus T_e .

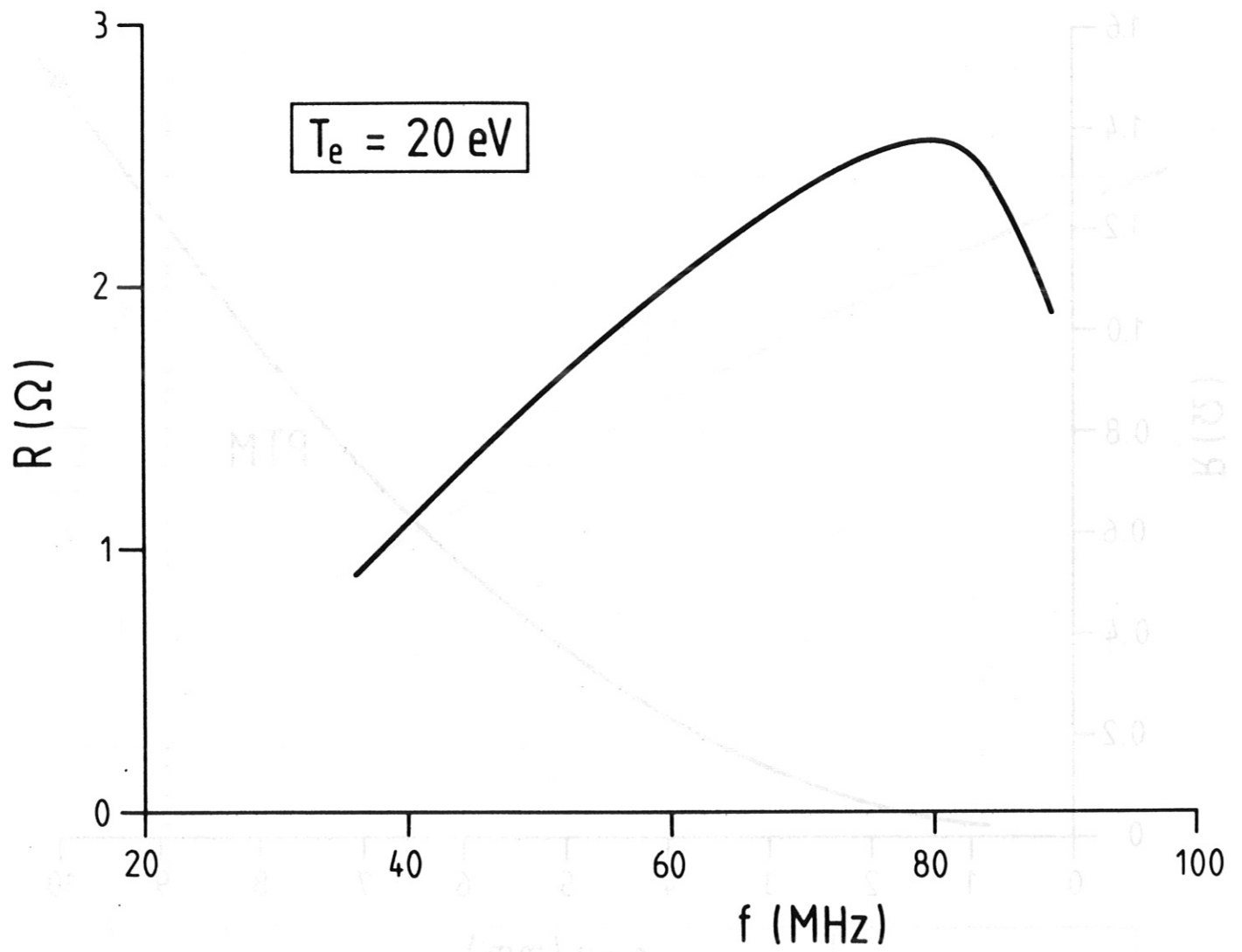


Fig.4 PTM loading versus f .

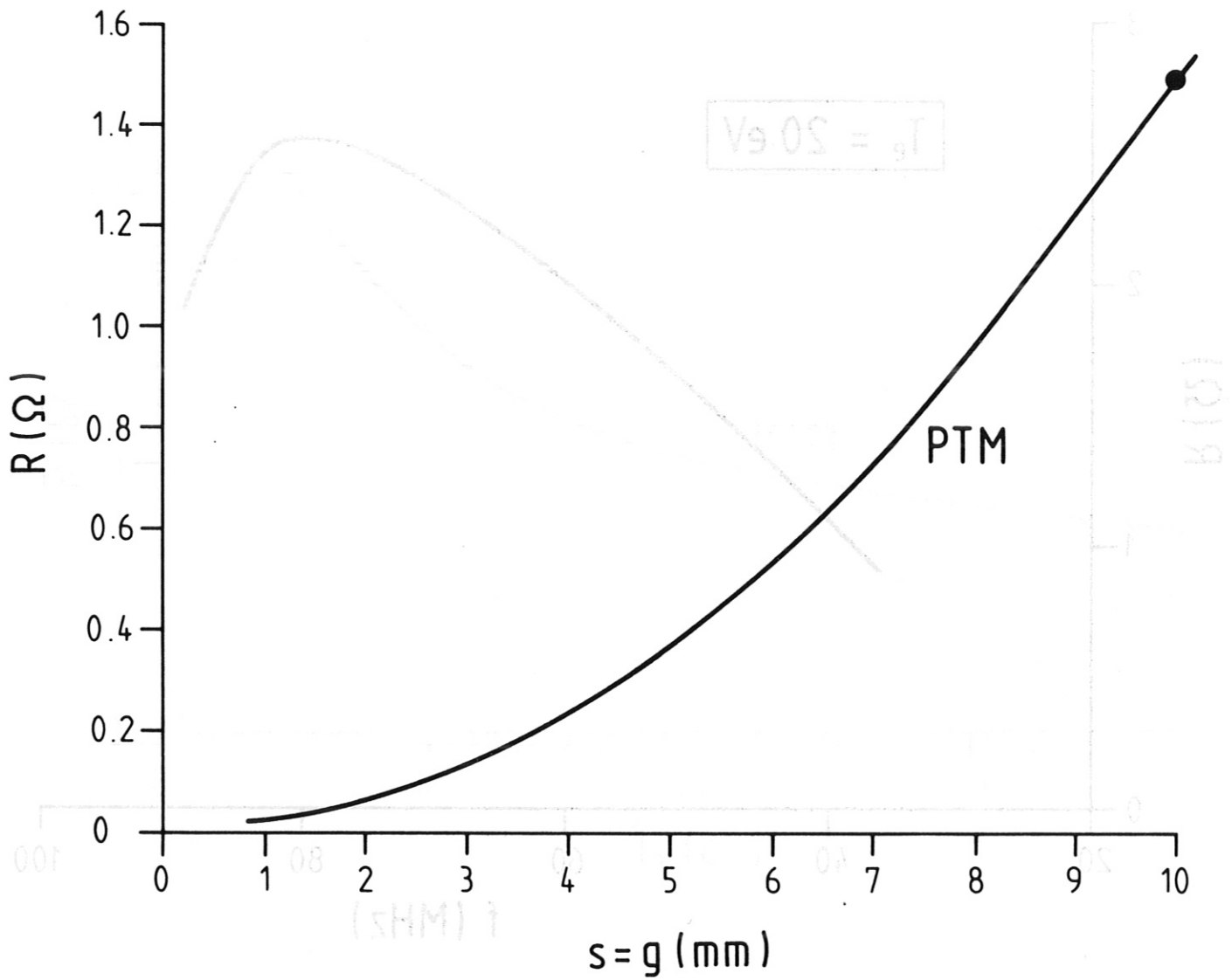


Fig.5 PTM loading vesus (s, g) .

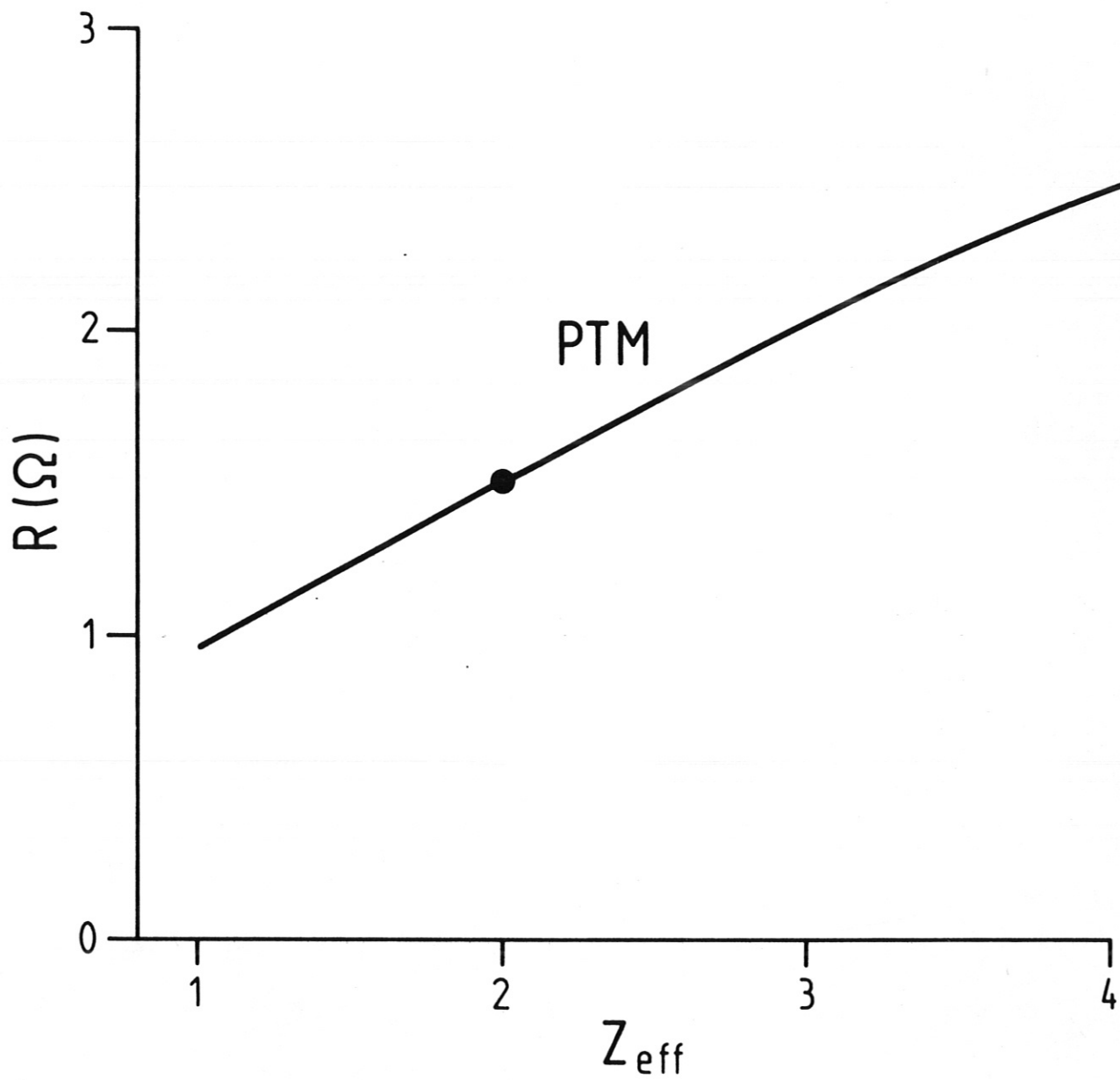


Fig.6 PTM loading versus Z_{eff} .